



Ba(B₂OF₃(OH)₂)₂ with well-ordered OH/F anions and a unique B₂OF₃(OH)₂ dimer†

 Cite this: *Chem. Commun.*, 2020, 56, 3301

 Received 22nd August 2019,
Accepted 10th February 2020

DOI: 10.1039/c9cc06532f

rsc.li/chemcomm

 Mingqiang Gai,^{‡,ab} Ying Wang,^{‡,a} Tinghao Tong,^{ab} Liying Wang,^c Zhihua Yang,^{id a}
Xin Zhou,^{id c} and Shilie Pan,^{id *a}

In minerals and artificial crystals, the OH and F groups often coexist and have a high probability of disordered structure. The OH/F position cannot be determined accurately in the crystal structure only by the direct X-ray diffraction method because of the poor contrast between O and F and the weak diffractivity of hydrogen atoms. In this work, a new fluorooxoborate Ba[B₂OF₃(OH)₂]₂, with a size of up to 12 × 4 × 3 mm³, has been synthesized successfully by a facile hydrothermal reaction. The BOF₃ units with well-ordered OH/F positions are observed for the first time in alkali/alkaline earth metal fluorooxoborates. Owing to the selective fluorination of BO₄, Ba(B₂OF₃(OH)₂)₂ exhibits a large birefringence and hence can be used as a DUV birefringent material. This work will guide the study of the structural chemistry of oxyfluorides.

Tailoring properties by incorporating mixed-anionic species into a crystal is expected to accelerate the discovery of new functional materials, and the applicability of this strategy has made great progress in many areas, *e.g.*, catalysis, energy conversion, and electronic devices.¹ Specifically, ordering of two or more anions within a mixed-anion compound often leads to low dimensionality in structural and intriguing physical properties which causes unanticipated responses to external stimuli.² For example, oxyfluorides with mixed-anionic species [MO_xF_y], such as [BO_xF_{4-x}]^{(x+1)-} (*x* = 1, 2, 3), MOF₅²⁻ (*M* = V, Nb, Ta), MO₂F₄²⁻ (*M* = Mo, W), MO₃F³⁻ (*M* = Se, Te), fluoriodates,

fluorophosphates, fluorosilicates and fluorosulfates, have been well achieved by different synthetic routes.³ Indeed, substitutions of oxygen by fluorine in oxides not only enable well-ordered anions in the crystal structure but also reduce the anionic dimensions and increase the freedom of the anionic framework.⁴ In addition, ordered anionic species in mixed anion compounds are of vital importance because of the correlation between crystal structure and physical properties.^{1b,c,2,3b} For example, the formation of [BO_xF_{4-x}]^{(x+1)-} (*x* = 1, 2, 3) in borates will be helpful for enlarging the bandgap and the local polarizability or hyperpolarizability.⁵ Thus, the fluorine-containing metal borates often possess unique functions when applied in nonlinear optics,⁶ ionic conduction, fluorescence,⁷ *etc.* However, in mixed-anion compounds, compared with anion-ordered ones, there are a considerable number of structures containing randomly disordered anions which are commonly found in minerals and artificial crystals according to the Inorganic Crystal Structure Database (ICSD). The attempt of “controlling” anion order and disorder is still a challenge, especially the presence of mixed F and OH groups.⁸ Only a handful of compounds with distinguishable OH/F positions, such as Hg₂(OH)[BF₄],⁹ (NH₃OH)_xMF_y (*M* = Ga, In, Sc, Mn, Cr, V, Co, Cu, Zn, Fe)¹⁰ and [HNC₆H₆OH]₂[Cu(NC₅H₅)₄(WO₂F₄)₂],^{3c} have been reported; however, there is scant evidence that the mixed OH/F species are ordered.

In this study, we report a new fluorooxoborate compound, Ba[B₂OF₃(OH)₂]₂ (BBOFH), containing a unique B₂OF₃(OH)₂ dimer. More than 29 fluorooxoborates have been reported to date, and 16 kinds of oxyfluoride FBBs and anionic frameworks of fluorooxoborate crystals are reported (Fig. S5, ESI†).¹¹ Although most of these fluorooxoborates also have a regular arrangement of F, the title compound is more specific in that both OH and F coexist simultaneously and are well-ordered on the tetrahedral and triangular ligands, respectively, which is relatively rare. The BOF₃ unit was also discovered for the first time in alkali/alkaline earth metal fluorooxoborates to the best of our knowledge. The method of determining the positions of OH and F was systematically discussed.

The BBOFH crystal with a size of up to 12 × 4 × 3 mm³ was grown by the facile hydrothermal growth method. The BBOFH

^a CAS Key Laboratory of Functional Materials and Devices for Special Environments, Xinjiang Technical Institute of Physics & Chemistry, CAS, Xinjiang Key Laboratory of Electronic Information Materials and Devices, 40-1 South Beijing Road, Urumqi 830011, China. E-mail: slpan@ms.xjb.ac.cn

^b Center of Materials Science and Optoelectronics Engineering, University of Chinese Academy of Sciences, Beijing 100049, China

^c Key Laboratory of Magnetic Resonance in Biological Systems, State Key Laboratory of Magnetic Resonance and Atomic and Molecular Physics, National Center for Magnetic Resonance in Wuhan, Wuhan Institute of Physics and Mathematics, CAS, Wuhan 430071, China

† Electronic supplementary information (ESI) available: Synthesis, crystallographic studies, characterization, and computational descriptions. CCDC 1952328. For ESI and crystallographic data in CIF or other electronic format see DOI: 10.1039/c9cc06532f

‡ These authors contributed equally to this work.

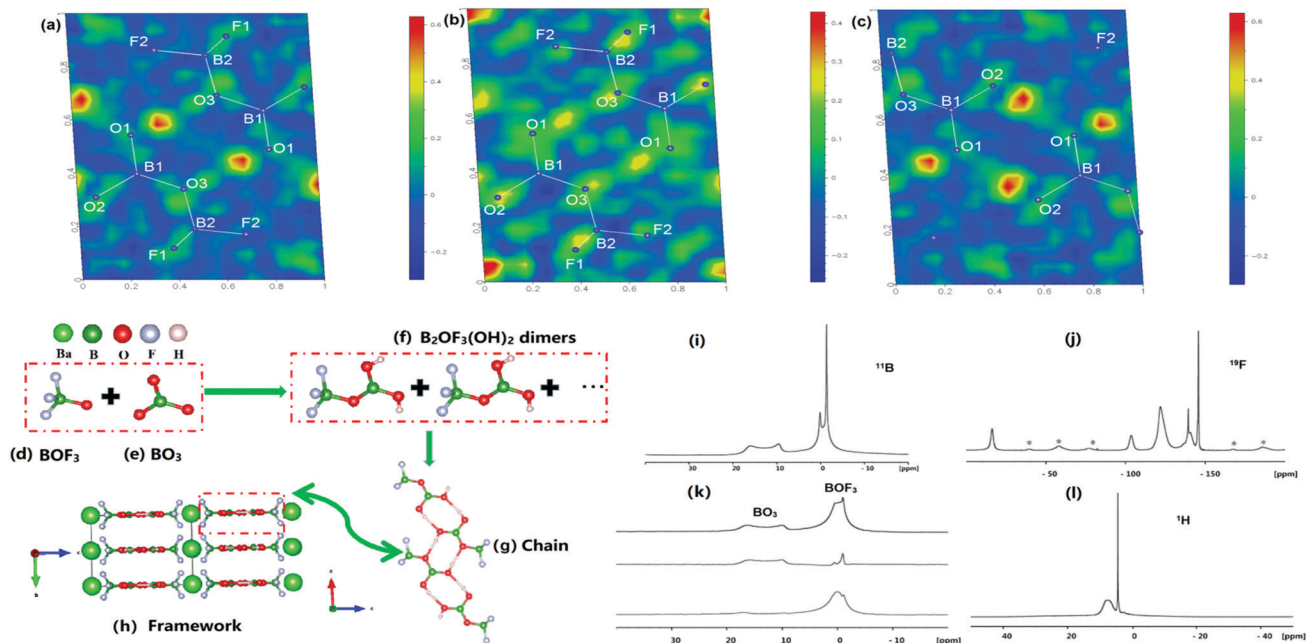


Fig. 1 Unbiased $F_o - F_c$ difference electron density maps of BBOFH (a–c). The most positive difference peaks (red) indicate the possible hydrogen atom positions. Crystal structures of BBOFH (d–h) and ^{11}B , ^{19}F , $^{11}\text{B}(^{19}\text{F})$ -REDOR and ^1H MAS NMR spectra of BBOFH (i–l).

crystal data were obtained at 153 K. BBOFH crystallizes in the centrosymmetric space group $C2/m$ (No. 12) of the monoclinic system with the unit cell parameters of $a = 6.803(3)$ Å, $b = 7.008(2)$ Å, $c = 9.588(3)$ Å, $\beta = 92.960(4)^\circ$, and $Z = 2$. The unbiased $F_o - F_c$ difference electron density maps (model without hydrogen) obtained from single-crystal data are given in Fig. 1a–c. The positive difference peaks clearly indicate the possible positions of hydrogen atoms around the O1 and O2 atoms, while no difference peaks were found near the F atoms, which provides primary evidence for the B–F and O–H bonds. The positions of the O and F atoms were also verified by bond valence calculation (BVS) (Table S2, ESI †),¹² which shows that the valences of Ba (2.089), O (1.873–2.087), F (0.964–1.068) and B (3.029–3.132) are reasonable. In addition, the structure model was checked by Neutron powder diffraction Rietveld refinement (Fig. S17, ESI †).

As shown in Fig. 1d–h, the fundamental building block (FBB) of BBOFH is the $\text{B}_2\text{OF}_3(\text{OH})_2$ group, which is composed of the $\text{BO}(\text{OH})_2$ triangle and the BOF_3 tetrahedron bridged by the O3 atom, and the $\text{B}_2\text{OF}_3(\text{OH})_2$ groups are linked with each other by hydrogen bonding to form a 1D $[\text{B}_2\text{OF}_3(\text{OH})_2]$ short chain. The parallel $[\text{B}_2\text{OF}_3(\text{OH})_2]$ chains extend along the b and c axes with the Ba1 cations located between two adjacent chains. In general, as the ratio of F:O increases, there is a higher possibility for the anionic framework in fluorooxoborates to be low-dimensional.¹³ BBOFH also follows this rule. The Ba1 atoms locate in a distorted icosahedron coordinated by oxygen and fluorine atoms. Specifically, the Ba^{2+} cations interact with two F2, eight F1 atoms and two O2 atoms with the Ba–F and Ba–O bond lengths of 2.780–2.916 and 2.879 Å, respectively (Fig. S3, ESI †). In the structure, all boron atoms show two types of coordination environments, forming the $\text{BO}(\text{OH})_2$ triangles

and the BOF_3 tetrahedra with the B–O and B–F bond lengths of 1.361–1.421 and 1.388–1.429 Å, respectively (Table S5, ESI †). The B–O/F bond lengths and the O–B–O/F angles are also comparable to those in recently reported fluorooxoborates.^{5a,13b,d,e,14}

The presence of hydroxyl, BO_3 and BOF_3 groups can be confirmed by the IR spectrum (Fig. S7, ESI †). According to the literature,^{13e,14f,15} the peaks at around 3321, 3229, 2972 and 1618 cm^{-1} exhibit the presence of hydroxyl groups. The bands in the range of 1454 and 962 cm^{-1} belong to asymmetric and symmetric stretching of the BO_3 groups. In particular, the asymmetric stretching of the B–F bonds is found in the range of 1387–993 cm^{-1} and the symmetric out of phase stretching of the B–F bonds is also found at 895 cm^{-1} . Besides, the bending vibrations of B–O can be observed at 773–563 cm^{-1} . The elemental distribution map shows that Ba, B, O and F are dispersed in BBOFH (Fig. S8, ESI †). This result further verifies that fluorine indeed exists in BBOFH.

In order to verify the presence of chemical bonds between the B and O/F atoms in BBOFH, we obtained the ^{11}B , ^{19}F and ^1H magic angle spinning (MAS) solid state nuclear magnetic resonance (NMR) spectra (Fig. 1i, j and l). In the ^{19}F MAS NMR spectrum (Fig. 1j), according to Höpfe and Kemnitz,^{13f,14f,15a} the signal at –16.3 ppm may be assigned to F nearest to Ba and the signals at –103.6, –121.96, –140.38, –140.69 and –145.82 ppm are assigned to F in the B–F groups. In the ^{19}F MAS NMR spectrum, we also find two dominant signals at –140.38 and –145.82 ppm, which are similar to the data in $\text{BaB}_4\text{O}_6\text{F}_2$, which again confirms the presence of B–F bonds in BBOFH. In the ^{11}B MAS NMR spectrum, the BO_3 chemical shifts often occur in the range of ~12.7–19.0 ppm,¹⁶ while the boron in the tetrahedral coordination shifts usually occur at around 0 ppm. In the ^{11}B MAS NMR spectrum (Fig. 1i), the broad signal ranging from 8 to 19 ppm

can be assigned to boron in trigonal coordination to oxygen, whereas the narrow signals at -1.41 and 0.18 ppm can be assigned to the tetrahedral coordinated B atoms. The $^{11}\text{B}\{^{19}\text{F}\}$ -rotational echo double resonance (REDOR) experiments were performed to establish the B–F bonds for the tetrahedral $[\text{BOF}_3]^{2-}$ units and the obtained different spectra clearly demonstrate that tetrahedrally coordinated B nuclei with the B–F bonds in BBOFH exist (Fig. 1k). The crystal structure of BBOFH has two unique H sites, and the H1 and H2 atoms are coordinated with the O1 and O2 atoms, respectively. The ^1H MAS NMR spectrum shows two resonances at $\delta = 4.3$ and 7.6 ppm (Fig. 1l), which are assigned to the H signals in the $\text{B}(\text{OH})_2$ groups with two different O–H distances. This further confirms the presence of the hydroxyl groups in BBOFH.

The ordering of F and OH can be understood by the bond valence model.^{3h,17} (1) The mean bond valences of the B–O bonds in BO_4 and BO_3 are 0.75 and 1, respectively. According to Pauling's second crystal rule (PSCR), a stable ionic structure is arranged to preserve local electroneutrality, so that the sum of the strengths of the electrostatic bond to an anion is equal to the charge on that anion.¹⁸ When hydroxyl competes with F, to have a relatively stable phase, compared to the BO_3 units, the BO_4 species are prone to connect with the F atoms with high electronegativity to reduce the bond valence of the B–O bonds. Thus, the reduced partial negative charge at the respective terminal oxygen and/or fluorine atoms in the fourfold coordination of the B atoms commonly acts as pinning sites for the cations.^{13g} Herein, the $[\text{BO}_x\text{F}_{4-x}]^{(x+1)-}$ ($x = 1, 2, 3$) groups should be more stable than the virtual $[\text{BO}_x\text{F}_{3-x}]^{x-}$ ($x = 1, 2$) groups in metal borates. As for fluorooxoborates containing both the BO_4 and BO_3 groups, the introduction of F will preferentially modify the BO_4 groups to form $[\text{BO}_x\text{F}_{4-x}]^{(x+1)-}$ ($x = 1, 2, 3$). $\text{LiB}_6\text{O}_9\text{F}$, $\text{Li}_2\text{B}_3\text{O}_4\text{F}_3$ and $\text{AB}_4\text{O}_6\text{F}$ ($\text{A} = \text{NH}_4, \text{Na}, \text{Rb}, \text{Cs}, \text{K/Cs}, \text{Rb/Cs}$) series are all typical examples.¹³ (2) Owing to the forceful electron accepting ability of the Ba atom, most of the F atoms with strong electronegativity tend to connect with Ba in the $\text{B}_2\text{OF}_3(\text{OH})_2$ groups. They may act as a scissor to “break” the layers of the B–O framework and further produce 1D short chains of $[\text{B}_2\text{OF}_3(\text{OH})_2]$. Therefore, if the hydroxyl groups in the $\text{BO}(\text{OH})_2$ triangles are partially or completely replaced by the F atoms, Ba will most likely connect with 11 or more fluorine atoms, and the virtual $[\text{B}_2\text{OF}_3(\text{OH})_{2-x}\text{F}_x]$ ($x = 1, 2$) groups will not link with each other by hydrogen bonding to form a 1D chain (Fig. S2, ESI†). This may lead to an unstable structure. Moreover, the phonon dispersion curves obtained by the first-principles calculations confirm that BBOFH has no negative frequencies and is dynamically stable, while the artificial “ $\text{Ba}[\text{B}_2\text{OF}_3(\text{OH})_{2-x}\text{F}_x]_2$ ($x = 1, 2$)” structures with mutual substitution of OH and F are not stable (Fig. S11, ESI†). Thus, the coexistence of $[\text{BOF}_3]^{2-}$ and the artificial $[\text{BO}_x\text{F}_{3-x}]^{x-}$ ($x = 1, 2$) groups in BBOFH will be difficult to achieve.

To check the thermal stability of BBOFH, thermogravimetry and differential scanning calorimetry (TG-DSC) were performed (Fig. S6, ESI†). There are three obvious endothermic peaks at around 282 , 697 and 803 °C on the TG curve for BBOFH. Almost 13.8% mass loss at around 282 °C is noticed, which may be

assigned to the part of removal of the BF_3 gas and the dehydration of the hydroxyls.^{15c,19}

The ultraviolet-visible-near-infrared transmittance spectrum of BBOFH was obtained in the ground crystals (Fig. S4, ESI†). The wide optical transmission spectrum (180 – 1200 nm) can be obtained in BBOFH. The first-principles calculations were performed by employing the CASTEP package. It was found that BBOFH has an indirect band gap of 8.35 eV (HSE06) by the PWmat code²⁰ (Fig. S10a, ESI†), which is comparable to that of the landmark deep-ultraviolet material $\text{KBe}_2\text{BO}_3\text{F}_2$ (KBBF) (8.43 eV).²¹ The total and partial densities of states (DOS and PDOS) of BBOFH are shown in Fig. S10b (ESI†). There are three energy parts from -9 to 9 eV, which show that the top of the VB and the bottom of the CB are mainly occupied by O-2p, B-2p and F-2p orbitals, revealing that the optical properties of BBOFH are mainly determined by the BOF_3 , BO_3 groups and d orbitals of the Ba atoms. The calculated birefringence of BBOFH is about 0.109 at 200 nm and 0.086 at 1064 nm, respectively (Fig. S9, ESI†). Considering the birefringence of α - BaB_2O_4 ($0.120@1064$ nm),²² KBBF ($0.080@1064$ nm)²¹ and the absorption edge of BBOFH lower than 180 nm, BBOFH may have potential applications in the deep-UV region. To better understand the origin of the birefringence in BBOFH, we investigated the material by the response electron distribution anisotropy (REDA) approximation method.²³ Based on the REDA analysis, the origin of birefringence in BBOFH is mainly attributed to the synergistic effect of BOF_3 (16.2%) and BO_3 (83.8%) groups. This indicates that the well-ordered OH/F group with regular arrangement makes a significant contribution for the large birefringence.

In summary, a new centimetre-scale fluorooxoborate crystal BBOFH, with a unique $\text{B}_2\text{OF}_3(\text{OH})_2$ dimer, has been obtained. It possesses well-ordered OH/F groups and exhibits a short ultraviolet cutoff edge (<180 nm), a large band gap (8.35 eV) and an appropriate birefringence ($0.109@200$ nm). The selective fluorination of the BO_4 groups mainly leads to the ordered OH/F groups in BBOFH. We also believe that the method of determining the positions of OH and F can provide a better theoretical basis for the study of hydrothermal synthesis of mixed anion compounds.

This work was supported by the National Natural Science Foundation of China (Grant No. 61835014 and 51425206), the Natural Science Foundation of Xinjiang (Grant No. 2016D01B061) and the National Key Research Project (Grant No. 2016YFB0402104). We thank Prof. Lunhua He and Dr Sihao Deng from State Key Laboratory for Magnetism, Institute of Physics, Chinese Academy of Sciences for their help in performing the Neutron powder diffraction experiment and analyzing the test results.

Conflicts of interest

There are no conflicts to declare.

Notes and references

- (a) J. Oró-Solé, L. Clark, W. Bonin, J. P. Attfield and A. Fuytes, *Chem. Commun.*, 2013, **49**, 2430–2432; (b) H. P. Wu, H. W. Yu, Z. H. Yang, X. L. Hou, X. Su, S. L. Pan, K. R. Poeppelmeier and J. M. Rondinelli,

- J. Am. Chem. Soc.*, 2013, **135**, 4215–4219; (c) N. Charles, R. J. Saballos and J. M. Rondinelli, *Chem. Mater.*, 2018, **30**, 3528–3537; (d) M. H. Yang, J. Oro-Solé, J. A. Rodgers, A. B. Jorge, A. Fuertes and J. P. Attfield, *Nat. Chem.*, 2010, **3**, 47–52; (e) J. L. Song, C. L. Hu, X. Xu, F. Kong and J. G. Mao, *Angew. Chem., Int. Ed.*, 2015, **54**, 3679–3682; (f) H. W. Yu, W. G. Zhang, J. Young, J. M. Rondinelli and P. S. Halasyamani, *Adv. Mater.*, 2015, **27**, 7380–7385; (g) M. L. Liang, C. L. Hu, F. Kong and J. G. Mao, *J. Am. Chem. Soc.*, 2016, **138**, 9433–9436; (h) F. F. Mao, C. L. Hu, X. Xu, D. Yan, B. P. Yang and J. G. Mao, *Angew. Chem., Int. Ed.*, 2017, **56**, 2151–2155; (i) T. T. Tran, J. He, J. M. Rondinelli and P. S. Halasyamani, *J. Am. Chem. Soc.*, 2015, **137**, 10504–10507; (j) X. Dong, L. Huang, C. Hu, H. Zeng, Z. Lin, X. Wang, K. M. Ok and G. H. Zou, *Angew. Chem., Int. Ed.*, 2019, **58**, 6528–6534; (k) J. Chen, C. L. Hu, F. F. Mao, J. H. Feng and J. G. Mao, *Angew. Chem., Int. Ed.*, 2019, **58**, 2098–2102; (l) T. D. Boyko, C. E. Zvoriste, I. Kinski, R. Riedel, S. Hering, H. Huppertz and A. Moewes, *Phys. Rev. B: Condens. Matter Mater. Phys.*, 2011, **84**, 085203.
- 2 H. Kageyama, K. Hayashi, K. Maeda, J. P. Attfield, Z. Hiroi, J. M. Rondinelli and K. R. Poeppelmeier, *Nat. Commun.*, 2018, **9**, 772.
- 3 (a) F. G. You, P. F. Gong, F. Liang, X. X. Jiang, H. Tu, Y. Zhao, Z. G. Hu and Z. S. Lin, *CrystEngComm*, 2019, **21**, 2485–2489; (b) M. R. Marvel, J. Lesage, J. Baek, P. S. Halasyamani, C. L. Stern and K. R. Poeppelmeier, *J. Am. Chem. Soc.*, 2007, **129**, 13963–13969; (c) M. E. Welk, A. J. Norquist, C. L. Stern and K. R. Poeppelmeier, *Inorg. Chem.*, 2001, **40**, 5479–5480; (d) H. W. Yu, M. L. Nisbet and K. R. Poeppelmeier, *J. Am. Chem. Soc.*, 2018, **140**, 8868–8876; (e) M. D. Donakowski, R. Gautier, H. Lu, T. T. Tran, J. R. Cantwell, P. S. Halasyamani and K. R. Poeppelmeier, *Inorg. Chem.*, 2015, **54**, 765–772; (f) D. Q. Jiang, G. P. Han, Y. Wang, H. Li, Z. H. Yang and S. L. Pan, *Inorg. Chem.*, 2019, **58**, 3596–3600; (g) B. B. Zhang, G. P. Han, Y. Wang, X. L. Chen, Z. H. Yang and S. L. Pan, *Chem. Mater.*, 2018, **30**, 5397–5403; (h) G. P. Han, B. H. Lei, Z. H. Yang, Y. Wang and S. L. Pan, *Angew. Chem., Int. Ed.*, 2018, **57**, 9828–9832; (i) M. Zhang, X. Su, M. Mutailipu, Z. H. Yang and S. L. Pan, *Chem. Mater.*, 2017, **29**, 945–949; (j) B. Ahmed, H. Jo, S.-J. Oh and K. M. Ok, *Inorg. Chem.*, 2018, **57**, 6702–6709.
- 4 G. P. Han, Y. Wang, B. B. Zhang and S. L. Pan, *Chem. – Eur. J.*, 2018, **24**, 17638–17650.
- 5 (a) R. H. Cong, Y. Wang, L. Kang, Z. Y. Zhou, Z. S. Lin and T. Yang, *Inorg. Chem. Front.*, 2015, **2**, 170–176; (b) S. L. Pan, Y. Wang and K. R. Poeppelmeier, *Photonic and Electronic Properties of Fluoride Materials*, 2016, pp. 311–354.
- 6 (a) S. Y. Niu, G. Joe, H. Zhao, Y. C. Zhou, T. Orvis, H. Huyan, J. Salman, K. Mahalingam, B. Urwin, J. B. Wu, Y. Liu, T. E. Tiwald, S. B. Cronin, B. M. Howe, M. Mecklenburg, R. Haiges, D. J. Singh, H. Wang, M. A. Kats and J. Ravichandran, *Nat. Photonics*, 2018, **12**, 392–396; (b) L. H. Nicholls, F. J. Rodríguez-Fortuño, M. E. Nasir, R. M. Córdova-Castro, N. Olivier, G. A. Wurtz and A. V. Zayats, *Nat. Photonics*, 2017, **11**, 628–633; (c) A. Tagaya, H. Ohkita, M. Mukoh, R. Sakaguchi and Y. Koike, *Science*, 2003, **301**, 812–814; (d) K. M. Ok, *Acc. Chem. Res.*, 2016, **49**, 2774–2785; (e) S. Schönegger, S. G. Jantz, A. Saxer, L. Bayarjargal, B. Winkler, F. Pielhofer, H. A. Höpfe and H. Huppertz, *Chem. – Eur. J.*, 2018, **24**, 16036–16043; (f) H. Huppertz and D. A. Keszler, *Borates: Solid-state Chemistry in Encyclopedia of Inorganic and Bioinorganic Chemistry*, John Wiley & Sons, Ltd, 2014, pp. 1–12; (g) P. S. Halasyamani and K. R. Poeppelmeier, *Chem. Mater.*, 1998, **10**, 2753–2769; (h) T. T. Tran, H. Yu, J. M. Rondinelli, K. R. Poeppelmeier and P. S. Halasyamani, *Chem. Mater.*, 2016, **28**, 5238–5258; (i) K. M. Ok, E. O. Chi and P. S. Halasyamani, *Chem. Soc. Rev.*, 2006, **35**, 710–717.
- 7 K. Swapna, S. Mahamuda, A. Srinivasa Rao, M. Jayasimhadri, T. Sasikala and L. Rama Moorthy, *Ceram. Int.*, 2013, **39**, 8459–8465.
- 8 (a) X. Y. Tang, J. X. Mi, R. C. Zhuang, S. H. Wang, S. F. Wu, Y. M. Pan and Y. X. Huang, *Inorg. Chem.*, 2019, **58**, 4508–4514; (b) S. Wang, E. V. Alekseev, J. Diwu, H. M. Miller, A. G. Oliver, G. Liu, W. Depmeier and T. E. Albrecht-Schmitt, *Chem. Mater.*, 2011, **23**, 2931–2939; (c) A. Ertl, R. Schuster, J. M. Hughes, T. Ludwig, H.-P. Meyer, F. Finger, M. D. Dyar, K. Ruschel, G. R. Rossman, U. Klötzli, F. Brandstätter, C. L. Lengauer and E. Tillmanns, *Eur. J. Mineral.*, 2012, **24**, 695–715; (d) G. Corbel, E. Suard, J. Emery and M. Leblanc, *J. Alloys Compd.*, 2000, **305**, 49–57; (e) M. Glätzle, A. Pitscheider, O. Oeckler, K. Wurst and H. Huppertz, *Chem. – Eur. J.*, 2019, **25**, 1767–1772.
- 9 D. Göbbels and G. Meyer, *Z. Anorg. Allg. Chem.*, 2003, **629**, 933–935.
- 10 (a) M. Kristl, B. Dojer, N. Hojnik and A. Golobič, *J. Fluorine Chem.*, 2014, **166**, 15–21; (b) M. Kristl, B. Dojer, M. Kasunič, A. Golobič, Z. Jagličič and M. Drogenik, *J. Fluorine Chem.*, 2010, **131**, 907–914; (c) B. Dojer, A. Golobič, Z. Jagličič, M. Kristl and M. Drogenik, *Monatsh. Chem.*, 2012, **143**, 175–180; (d) M. Kristl, B. Volavsek and L. Golic, *Monatsh. Chem.*, 1996, **127**, 581–586.
- 11 C. M. Huang, F. F. Zhang, H. Li, Z. H. Yang, H. H. Yu and S. L. Pan, *Chem. – Eur. J.*, 2019, **25**, 6693–6697.
- 12 N. E. Brese and M. O’Keeffe, *Acta Crystallogr., Sect. B: Struct. Sci.*, 1991, **B47**, 192–197.
- 13 (a) Y. Wang, B. B. Zhang, Z. H. Yang and S. L. Pan, *Angew. Chem., Int. Ed.*, 2018, **57**, 2150–2154; (b) X. L. Chen, B. L. Zhang, F. F. Zhang, Y. Wang, M. Zhang, Z. H. Yang, K. R. Poeppelmeier and S. L. Pan, *J. Am. Chem. Soc.*, 2018, **140**, 16311–16319; (c) B. B. Zhang, G. Q. Shi, Z. H. Yang, F. F. Zhang and S. L. Pan, *Angew. Chem., Int. Ed.*, 2017, **56**, 3916–3919; (d) X. F. Wang, Y. Wang, B. B. Zhang, F. F. Zhang, Z. H. Yang and S. L. Pan, *Angew. Chem., Int. Ed.*, 2017, **56**, 14119–14123; (e) G. Q. Shi, Y. Wang, F. F. Zhang, B. B. Zhang, Z. H. Yang, X. L. Hou, S. L. Pan and K. R. Poeppelmeier, *J. Am. Chem. Soc.*, 2017, **139**, 10645–10648; (f) T. Bräuniger, T. Pilz, C. V. Chandran and M. Jansen, *J. Solid State Chem.*, 2012, **194**, 245–249; (g) T. Pilz, H. Nuss and M. Jansen, *J. Solid State Chem.*, 2012, **186**, 104–108.
- 14 (a) Z. Z. Zhang, Y. Wang, B. B. Zhang, Z. H. Yang and S. L. Pan, *Inorg. Chem.*, 2018, **57**, 4820–4823; (b) C. C. Tang, X. X. Jiang, W. L. Yin, L. J. Liu, M. J. Xia, Q. Huang, G. M. Song, X. Y. Wang, Z. S. Lin and C. T. Chen, *Dalton Trans.*, 2019, **48**, 21–24; (c) S. J. Han, B. B. Zhang, Z. H. Yang and S. L. Pan, *Chem. – Eur. J.*, 2018, **24**, 10022–10027; (d) Z. Z. Zhang, Y. Wang, B. B. Zhang, Z. H. Yang and S. L. Pan, *Angew. Chem., Int. Ed.*, 2018, **57**, 6577–6581; (e) M. Mutailipu, M. Zhang, B. B. Zhang, L. Y. Wang, Z. H. Yang, X. Zhou and S. L. Pan, *Angew. Chem., Int. Ed.*, 2018, **57**, 6095–6099; (f) M. Mutailipu, M. Zhang, B. B. Zhang, Z. H. Yang and S. L. Pan, *Chem. Commun.*, 2018, **54**, 6308–6311; (g) G. P. Han, G. Q. Shi, Y. Wang, B. B. Zhang, S. J. Han, F. F. Zhang, Z. H. Yang and S. L. Pan, *Chem. – Eur. J.*, 2018, **24**, 4497–4502.
- 15 (a) S. G. Jantz, F. Pielhofer, L. van Wüllen, R. Wehrich, M. J. Schäfer and H. A. Höpfe, *Chem. – Eur. J.*, 2018, **24**, 443–450; (b) C. M. Huang, F. F. Zhang, B. B. Zhang, Z. H. Yang and S. L. Pan, *New J. Chem.*, 2018, **42**, 12091–12097; (c) L. Y. Li, G. B. Li, Y. X. Wang, F. H. Liao and J. H. Lin, *Chem. Mater.*, 2005, **17**, 4174–4180; (d) S. Schönegger, K. Wurst, G. Heymann, A. Schaur, A. Saxer, D. Johrendt and H. Huppertz, *Z. Naturforsch. B*, 2018, **73**, 337–348.
- 16 (a) L. J. Todd, A. R. Siedle, F. Sato, A. R. Garber, F. R. Scholer and G. D. Mercer, *Inorg. Chem.*, 1975, **14**, 1249–1252; (b) G. L. Turner, K. A. Smith, R. J. Kirkpatrick and E. Oldfield, *J. Magn. Reson.*, 1986, **67**, 544–550.
- 17 I. D. Brown, *Chem. Rev.*, 2009, **109**, 6858–6919.
- 18 (a) A. Fuertes, *Inorg. Chem.*, 2006, **45**, 9640–9642; (b) L. Pauling, *J. Am. Chem. Soc.*, 1929, **51**, 1010–1026.
- 19 J. H. Huang, C. C. Jin, P. L. Xu, P. Gong, Z. Lin, J. W. Cheng and G.-Y. Yang, *Inorg. Chem.*, 2019, **58**, 1755–1758.
- 20 (a) W. L. Jia, J. Y. Fu, Z. Y. Cao, L. Wang, X. B. Chi, W. G. Gao and L. W. Wang, *J. Comput. Phys.*, 2013, **251**, 102–115; (b) W. L. Jia, Z. Y. Cao, L. Wang, J. Y. Fu, X. B. Chi, W. G. Gao and L. W. Wang, *Comput. Phys. Commun.*, 2013, **184**, 9–18.
- 21 C. T. Chen, G. L. Wang, X. Y. Wang and Z. Y. Xu, *Appl. Phys. B: Lasers Opt.*, 2009, **97**, 9–25.
- 22 G. Q. Zhou, J. Xu, X. D. Chen, H. Y. Zhong, S. T. Wang, K. Xu, P. Z. Deng and F. X. Gan, *J. Cryst. Growth*, 1998, **191**, 517–519.
- 23 (a) C. Hu, B. B. Zhang, B. H. Lei, S. L. Pan and Z. H. Yang, *ACS Appl. Mater. Interfaces*, 2018, **10**, 26413–26421; (b) B. H. Lei, Z. H. Yang and S. L. Pan, *Chem. Commun.*, 2017, **53**, 2818–2821; (c) B. H. Lei, Z. H. Yang, H. W. Yu, C. Cao, Z. Li, C. Hu, K. R. Poeppelmeier and S. L. Pan, *J. Am. Chem. Soc.*, 2018, **140**, 10726–10733.